

Synergistic Sphere-to-Rod Micelle Transition in Mixed Solutions of Sodium Dodecyl Sulfate and Cocoamidopropyl Betaine

N. C. Christov,[†] N. D. Denkov,^{*,†} P. A. Kralchevsky,[†]
K. P. Ananthapadmanabhan,[‡] and A. Lips[‡]

Laboratory of Chemical Physics & Engineering, Faculty of Chemistry, Sofia University,
1164 Sofia, Bulgaria, and Unilever Research U.S., 45 River Road,
Edgewater, New Jersey 07020

Received September 14, 2003. In Final Form: November 18, 2003

Static and dynamic light scattering experiments show that the mixed micelles of sodium dodecyl sulfate (SDS) and cocoamidopropyl betaine (CAPB) undergo a sphere-to-rod transition at unexpectedly low total surfactant concentrations, about 10 mM. The lowest transition concentration is observed at molar fraction 0.8 of CAPB in the surfactant mixture. The transition brings about a sharp increase in the viscosity of the respective surfactant solutions due to the growth of rodlike micelles. Parallel experiments with mixed solutions of CAPB and sodium laureth sulfate (sodium dodecyl-trioxyethylene sulfate, SDP3S) showed that the sphere-to-rod transition in SDP3S/CAPB mixtures occurs at higher surfactant concentrations, above 40 mM. The observed difference in the transition concentrations for SDS and SDP3S can be explained by the bulkier SDP3S headgroup. The latter should lead to larger mean area per molecule in the micelles containing SDP3S and, hence, to smaller spontaneous radius of curvature of the micelles (i.e., less favored transition from spherical to rodlike micelles). The static light scattering data are used to determine the mean aggregation number and the effective size of the spherical mixed SDS/CAPB micelles. From the dependence of the aggregation number on the surfactant concentration, the mean energy for transfer of a surfactant molecule from a spherical into a rodlike micelle is estimated.

1. Introduction

Mixed solutions of anionic and zwitterionic surfactants are used in various detergent formulations because of their superior properties in comparison to the properties of individual surfactants.^{1–3} For example, mixed solutions often have lower critical micelle concentration (cmc) due to a strong attraction between the molecules of the anionic and zwitterionic surfactants.^{1–8} The low cmc is beneficial in the case of facial cleansers, shampoos, and baby-care products, because it leads to a reduced irritation action of the surfactant solution on the eyes and skin.^{1–3} In addition, the mixed solutions often have improved foaming, emulsifying, and rheological properties, at the same total surfactant concentration, which are important for their applications.^{1–3,8–10}

Alkylbetaines and their derivatives represent a class of zwitterionic surfactants, which are electroneutral inner salts in a wide pH range, with a positive charge on the nitrogen atom and a negative charge on the carboxyl group. Alkylbetaines and alkylamidobetaines are among the most widely used cosurfactants in mixtures with anionic surfactants, such as sodium dodecyl sulfate (SDS) and various sodium laureth sulfates (with 2, 3, or 4 ethoxy groups), especially in shampoos and liquid detergents, because they have pronounced foam/lather boosting, antistatic, and hair-conditioning effects. Betaines also find industrial applications in textile production (mainly due to their antistatic and softening properties) and as emulsifiers and dispersants, for example, for photographic emulsions.^{1–3}

In relation to the above applications, mixtures of alkylbetaines and anionic surfactants have been investigated to understand the phenomena that are responsible for the synergistic action of these systems. Rosen and co-workers^{4,11,12} characterized the adsorption layers and micelles in mixed surfactant systems in terms of the so-called molecular interaction parameters (MIPs). These authors^{4,11,12} found that MIPs are strongly negative for mixtures of anionic surfactants and betaines, indicating a significant intermolecular attraction (see Figure 1). The molecular interactions of betaines with anionic surfactants were studied also, in relation to other properties of the surfactant mixtures, which are important for their applications (e.g., Kraft temperature).^{5,13–16} Iwasaki et al.⁸

* To whom correspondence should be addressed. Assoc. Prof. Nikolai D. Denkov, Laboratory of Chemical Physics & Engineering, Faculty of Chemistry, Sofia University, 1 James Bourchier Ave., 1164 Sofia, Bulgaria. Phone: (+359-2) 962 5310. Fax: (+359-2) 962 5643. E-mail: ND@LCPE.UNI-SOFIA.BG.

[†] Sofia University.

[‡] Unilever Research U.S.

(1) *Amphoteric Surfactants*; Lomax, E. G., Ed.; Surfactant Science Series, Vol. 59; Marcel Dekker: New York, 1996.

(2) Domingo, X. In *Amphoteric Surfactants*; Lomax, E. G., Ed.; Surfactant Science Series, Vol. 59; Marcel Dekker: New York, 1996; Chapter 3.

(3) Tsujii, K. *Surface Activity: Principles, Phenomena, and Applications*; Academic Press: New York, 1998.

(4) Rosen, M. J. *Surfactants and Interfacial Phenomena*, 2nd ed.; Wiley-Interscience: New York, 1989.

(5) Holland, P.; Rubingh, D. N. *J. Phys. Chem.* **1983**, *87*, 1984. Holland, P. *Adv. Colloid Interface Sci.* **1986**, *26*, 111.

(6) Abe, M.; Kato, K.; Ogino, K. *J. Colloid Interface Sci.* **1989**, *127*, 329.

(7) Shiloach, A.; Blankshtein, D. *Langmuir* **1997**, *13*, 3968. Mulqueen, M.; Blankshtein, D. *Langmuir* **2000**, *16*, 7640.

(8) Iwasaki, T.; Ogawa, M.; Esumi, K.; Meguro, K. *Langmuir* **1991**, *7*, 30.

(9) Basheva, E. S.; Ganchev, D.; Denkov, N. D.; Kasuga, K.; Satoh, N.; Tsujii, K. *Langmuir* **2000**, *16*, 1000.

(10) Basheva, E. S.; Stoyanov, S.; Denkov, N. D.; Kasuga, K.; Satoh, N.; Tsujii, K. *Langmuir* **2001**, *17*, 969.

(11) Rosen, M. J.; Zhu, Z. H. *J. Colloid Interface Sci.* **1984**, *99*, 427, 435.

(12) Rosen, M. J.; Zhu, Z. H. *J. Am. Oil Chem. Soc.* **1988**, *65*, 663.

(13) Hines, J. D.; Thomas, R. K.; Garrett, P. R.; Rennie, G. K.; Penfold, J. *J. Phys. Chem. B* **1998**, *102*, 8834.

(14) Tajima, K.; Nakamura, A.; Tsutsui, T. *Bull. Chem. Soc. Jpn.* **1979**, *52*, 2060.

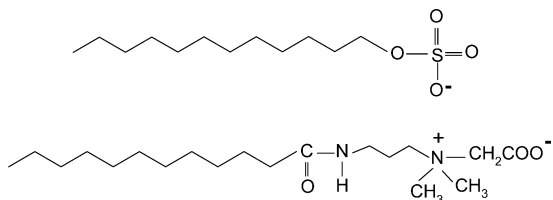


Figure 1. Schematic presentation of the electrostatic head-head attraction between SDS and CAPB molecules, incorporated in a micelle or adsorption layer.

studied mixtures of SDS and alkylbetaines and found that several properties of the surfactant blends (cmc, micelle aggregation number, diffusion coefficient, and solubilization capacity) strongly depend on the ratio of SDS/betaine and exhibit maxima or minima when the molar fraction of alkylbetaine in the mixture is about 0.6. These results were explained by strong electrostatic attraction between the SDS and alkylbetaine molecules in the mixed micelles and adsorption layers. A comprehensive review on this subject can be found in ref 2.

In the present paper, we describe a systematic light scattering study of the sphere-to-rod micelle transition in mixed solutions of cocoamidopropyl betaine (CAPB) and SDS. It is found that the transition in this system occurs at a rather low total surfactant concentration (≈ 10 mM) and is related to a sharp increase in the viscosity of the respective solutions. The data from light scattering are used to determine the micelle aggregation numbers and to evaluate the interaction between the SDS and CAPB molecules in the rodlike micelles. In addition, the light scattering data were used to characterize the micellar effective volume fraction in relation to the oscillatory surface forces, which are known to be operative in thin foam and emulsion films formed from micellar solutions.

2. Materials and Methods

2.1. Materials. SDS (99%, a product of ACROS Co., NJ) and sodium polyoxyethylene sulfate with three ethoxy groups (SDP3S) of commercial name STEOL CS-330 (a product of Stepan Co., Northfield, IL) were studied as anionic surfactants. CAPB of commercial name TEGO Betaine F 50 (a product of Golgschmidt Chemical Co., Hopewell, VA) was used as a zwitterionic surfactant. NaCl (a product of Merck KGaA, Darmstadt, Germany) was always added to the surfactant solutions in concentration of 10 mM, as a neutral electrolyte.

All solutions were prepared with deionized water from a Milli-Q water purification system (Millipore) in glassware, which was pre-cleaned by sulfochromic acid and rinsed with Millipore water. Just before performing the light scattering experiments, all samples were filtered through a 100 nm filter to remove dust particles (Millex VV, Millipore).

2.2. Methods. Dynamic light scattering (DLS) was used for measuring the translational diffusion coefficient, D , of the surfactant micelles. Then, the mass-averaged hydrodynamic diameter of the micelles, d_h , was calculated by using the Stokes-Einstein relation

$$d_h = kT/(3\pi\eta D) \quad (1)$$

where η is the dynamic viscosity of the disperse medium, T is temperature, and k is the Boltzmann constant.

Static light scattering (SLS) was used to determine the total mass, M_w , and the second virial coefficient, A_2 , of the spherical micelles (A_2 brings information about the interaction between

the micelles). The data from the SLS experiments were interpreted by using the Zimm plot (see, e.g., refs 17 and 18):

$$\frac{KC}{R(\theta)} = \frac{1}{M_w} \left[1 + \frac{16}{3} \left(\frac{\pi n}{\lambda_w} \right)^2 \sin^2(\theta/2) R_g^2 \right] + 2A_2C \quad (2)$$

where C is the total surfactant concentration in the solution (all experiments were performed with solutions having concentrations well above the cmc, so that the concentration of the monomers, which are not incorporated in micelles, can be neglected); $R(\theta)$ is the Rayleigh ratio, which is proportional to the intensity of the scattered light; θ is the scattering angle; R_g is the radius of gyration of the micelles (too small in the studied solutions to be reliably measured); λ_w is the wavelength of the illuminating light; K is an optical constant,

$$K = \frac{4\pi^2}{N_A} \frac{n_0^2}{\lambda_w^4} \left(\frac{dn}{dC} \right)^2 \quad (3)$$

N_A is the Avogadro number; n_0 is the refractive index of water; dn/dC is the refractive index increment, which is measured independently by a Pulfrich refractometer.

From M_w , we determined the aggregation number and composition of the spherical micelles, that is, the number of SDS and CAPB molecules per micelle, N_{SDS} and N_{CAPB} , by assuming that the ratio of SDS and CAPB in the micelles is the same as in the total surfactant mixture. The latter assumption is justified insofar as the studied solutions were of concentrations well above the cmc and the formation of two different micelle populations, enriched in SDS and CAPB, is not expected in the region of spherical micelles (due to the attraction between the SDS and CAPB molecules in the micelles). Thus, N_{SDS} and N_{CAPB} can be calculated from the relations $N_{SDS} = (1 - f_{CAPB})N_s$ and $N_{CAPB} = f_{CAPB}N_s$, where f_{CAPB} is the molar fraction of CAPB in the surfactant mixture and N_s is the total aggregation number of the spherical micelles, which is calculated from the Zimm plot:

$$N_s = M_w / [(1 - f_{CAPB})M_{SDS} + f_{CAPB}M_{CAPB}] \quad (4)$$

In eq 4, we have used the fact that the weight-averaged mass of the micelles can be expressed as $M_w = N_{SDS}M_{SDS} + N_{CAPB}M_{CAPB}$, where M_{SDS} or M_{CAPB} is the molecular mass of SDS or CAPB, respectively.

Note that the aggregation number of the rodlike micelles, N_R , was estimated from DLS data by using another procedure, explained in section 4 below, because eq 2 is not applicable in the region of rodlike micelles and M_w cannot be determined from the Zimm plot (see section 3.2 for further explanations).

The light scattering measurements were performed at 27 °C by means of an instrument 4700C (Malvern Instruments, U.K.), which is equipped with an argon laser, operating with a vertically polarized incident beam at $\lambda_w = 488$ nm.

The viscosity of the solutions was measured by means of a capillary viscometer thermostated at 27 ± 0.2 °C.

3. Experimental Results and Discussion

3.1. Concentration of Sphere-to-Rod Transition and Relation to Solution Viscosity. The DLS measurements with surfactant mixtures (at fixed ratio SDS/CAPB) showed a well-pronounced transition in the size of the mixed micelles at a certain total concentration of surfactant, C_{SR} . At low surfactant concentrations, the hydrodynamic diameter of the micelles was $d_h \approx 5$ nm for all studied systems, which corresponds to spherical micelles. In Figure 2A, illustrative results are presented for surfactant mixtures with molar fraction of CAPB $f_{CAPB} = 0.5$ and 0.75. After the break point in the curve of d_h

(15) Wüstneck, R.; Miller, R.; Kriwanek, J.; Holzbauer, H.-R. *Langmuir* **1994**, *10*, 3738.

(16) Tsujii, K.; Okahashi, K.; Takeuchi, T. *J. Phys. Chem.* **1982**, *86*, 1437.

(17) Mazer, N. A. In *Dynamic Light Scattering: Applications of Photon Correlation Spectroscopy*; Pecora, R., Ed.; Plenum Press: New York, 1985; Chapter 8.

(18) Kralchevsky, P. A.; Danov, K. D.; Denkov, N. D. In *Handbook of Surface and Colloid Chemistry*; Birdi, K. S., Ed.; CRC Press: New York, 1997, Chapter 11; 2nd ed., 2002, Chapter 5.

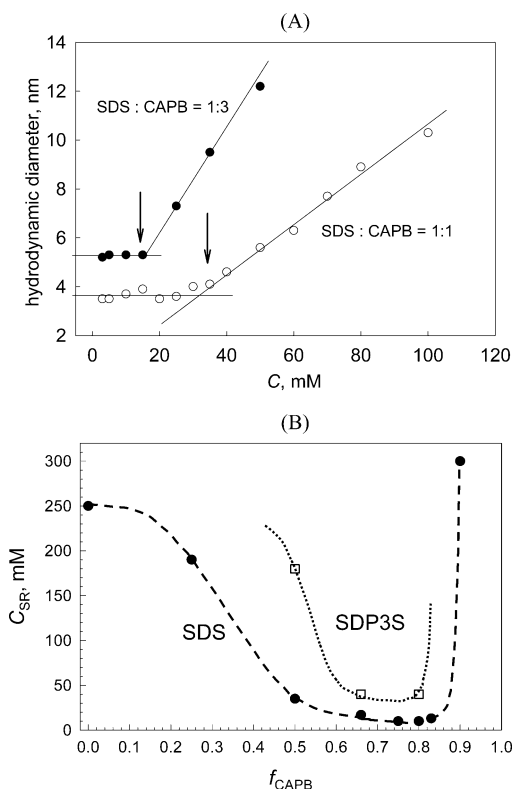


Figure 2. (A) Mean hydrodynamic diameter, d_h , of the micelles as determined by DLS in mixed SDS/CAPB solutions at two different ratios, 1:1 and 1:3. The arrows indicate the break-point concentrations in the respective Zimm plots, as determined by SLS. (B) Total surfactant concentration at the sphere-to-rod transition, C_{SR} , as a function of the molar fraction of CAPB in the mixture, f_{CAPB} . The circles correspond to mixtures of CAPB with SDS, whereas the empty squares are for mixtures with SDP3S. The curves are guides to the eye.

versus C , the size of the micelles rapidly increases and d_h becomes larger than 10 nm. For comparison, the size of the single-component SDS micelles^{17,19,20} is $d_h = 4.8$ nm and for the CAPB micelles we measured $d_h = 5.2 \pm 0.5$ nm in the entire concentration range shown in Figure 2A.

In Figure 2B, we plot the dependence of the transitional concentration, C_{SR} , on the molar fraction of CAPB in the mixture. One sees that the transition occurs at total surfactant concentrations as low as 10 mM, for CAPB molar fraction ≈ 0.8 . For comparison, the sphere-to-rod transition concentration in solutions of pure SDS occurs at about 250 mM,¹⁹ and our own measurements by DLS showed that there is no such transition for the studied CAPB even at concentrations as high as 500 mM. Hence, the sphere-to-rod transition in the mixed solutions occurs at total surfactant concentrations that are more than 1 order of magnitude lower than the transition concentrations for the individual surfactants.

Measurements with mixed surfactant solutions showed that their viscosity rapidly increased after the sphere-to-rod transition; see Figure 3A. As evidenced by the comparison of the micelle diameter and solution viscosity (see Figure 3B), the observed increase of viscosity is closely related to the increase of the micelle size after the transition. Note also that the maxima in the curves for the micelle size and solution viscosity (Figure 3B) correspond to the minimum in the curve C_{SR} versus f_{CAPB} shown in Figure 2B.

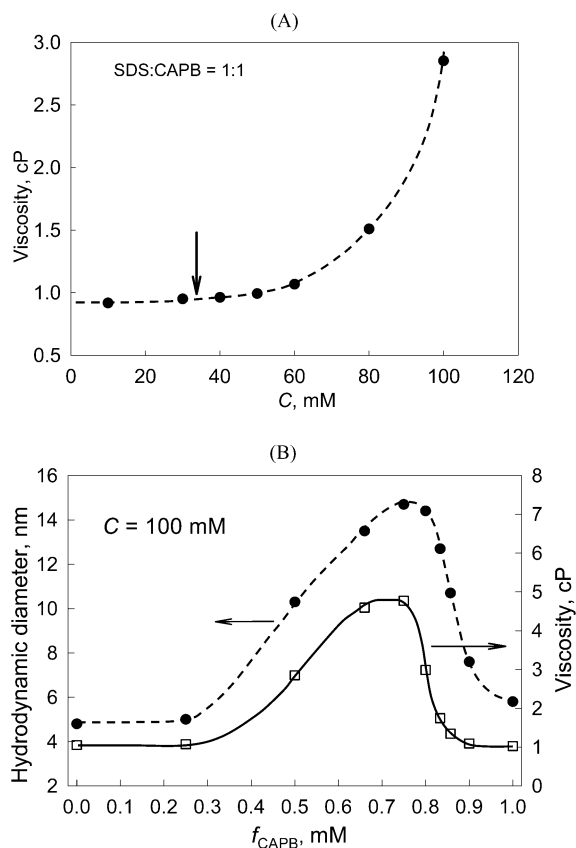


Figure 3. (A) Viscosity of the surfactant solutions containing SDS/CAPB = 1:1, as a function of the total surfactant concentration. The arrow corresponds to the sphere-to-rod transition, as determined by light scattering. (B) Dependence of the hydrodynamic diameter, d_h (circles), and of the solution viscosity (empty squares) on the molar fraction of CAPB in the surfactant mixture, f_{CAPB} , at total surfactant concentration $C = 0.1$ M.

Similar light scattering experiments were performed with mixed solutions of CAPB and SDP3S (another anionic surfactant used in practical formulations, which differs from SDS by the presence of three ethoxy groups in the surfactant head). The experiments showed that the sphere-to-rod transition in the SDP3S/CAPB mixture occurs at higher total surfactant concentrations, $C_{SR} > 40$ mM, as compared to the SDS/CAPB mixtures (see the dotted curve in Figure 2B).

The comparison of the results for SDS and SDP3S suggests that the additional ethoxy groups make the headgroup of SDP3S bulkier, as compared to SDS. As a result, the mean area per molecule in the micelles containing SDP3S is expected to be larger, which should lead to a smaller spontaneous radius of curvature of the micelles and, hence, to a less favored transition from spherical to rodlike micelles.

3.2. Aggregation Number, Second Virial Coefficient, Effective Diameter, and Effective Volume Fraction of the Spherical Micelles. In the Zimm plot, obtained by SLS, the transition in the micelle size (and the related increase of aggregation number) appears as a sharp break point in the data; see the example shown in Figure 4 for 0.75 molar fraction of CAPB in the surfactant mixture (similar results were obtained with the other mixed solutions). At low surfactant concentrations, the plot of the data has a positive slope; that is, the second virial coefficient, $A_2 > 0$, indicates a net repulsion between the spherical micelles formed in this concentration range. The negative slope in the SLS data, after the

(19) Reiss-Husson, F.; Luzzati, V. *J. Phys. Chem.* **1964**, *68*, 3504.

(20) Rohde, A.; Sackmann, E. *J. Colloid Interface Sci.* **1979**, *70*, 494.

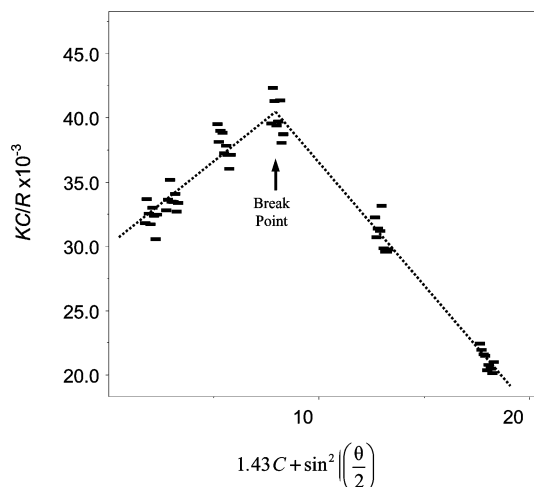


Figure 4. Zimm plot of the mixed solutions of SDS and CAPB at $f_{\text{CAPB}} = 0.75$. The dotted lines are guides to the eye.

break point, is due to the rapid increase of the micelle aggregation number at $C > C_{\text{SR}}$. Note that the data interpretation, by means of eq 2, is not justified beyond the break point, because eq 2 implies that the micelle size and shape do not depend on surfactant concentration, which is not the case for $C > C_{\text{SR}}$.

By using eqs 2–4, one can interpret the experimental data from the SLS experiments in the range of low surfactant concentrations (where only spherical micelles are present) and determine the micelle aggregation number, N_{S} , and the second virial coefficient, A_2 . The results from this analysis are summarized in Table 1. As seen from the table, the aggregation number of the *mixed* spherical micelles, $N_{\text{S}} \approx 113 \pm 5$, is larger than that of the micelles consisting of individual components, $N_{\text{SDS}} \approx 89$ and $N_{\text{CAPB}} \approx 84$, respectively. The larger size of the mixed micelles is probably related to the strong attraction between the SDS and CAPB headgroups, which probably decreases the mean area per molecule and thus favors the incorporation of more surfactant molecules per micelle.

All virial coefficients are positive in the studied systems, which indicates a net repulsion between the spherical micelles. As expected, the magnitude of A_2 increases with the fraction of SDS in the surfactant mixture, because SDS brings a negative charge to the micelles. The used batch of CAPB contained NaCl, which had a screening effect on the surface charge of the micelles (by measuring the electroconductivity of CAPB solutions, we determined that the concentration of NaCl in the batch sample was 7 wt % with respect to CAPB). This screening effect is more pronounced at the higher molar fractions of CAPB in the mixture, where more NaCl is introduced into the solutions. Therefore, the reduced virial coefficient at higher CAPB to SDS ratios is related to (1) reduced micelle charge and (2) more screened electrostatic repulsion between the micelles.

From the values of A_2 , one can determine the so-called effective volume of the micelles, V_{EFF} , which accounts for the micelle interactions:¹⁸

$$V_{\text{EFF}} = \frac{1}{8} \int_0^{\infty} [1 - \exp(-W(r)/kT)] 4\pi r^2 dr \quad (5)$$

where $W(r)$ is the interaction energy between two micelles separated at a center-to-center distance, r . For particles interacting as hard spheres, $V_{\text{EFF}} = V_{\text{S}}$. In contrast, V_{EFF} could be substantially different from the actual micelle volume, V_{S} , if long-range interactions between the particles are present.

As explained in ref 18, V_{EFF} can be expressed through the second osmotic virial coefficient measured by SLS:

$$V_{\text{EFF}} = \frac{1}{4} \frac{A_2 M_{\text{W}}^2}{N_{\text{A}}} \quad (6)$$

Further, from V_{EFF} and the aggregation number N_{S} we estimated the effective volume fraction of the micelles at the transition concentration,

$$\Phi_{\text{EFF}}(C_{\text{SR}}) = \rho_{\text{SR}} V_{\text{EFF}} = \frac{C_{\text{SR}} N_{\text{A}}}{N_{\text{S}}} V_{\text{EFF}} \quad (7)$$

where ρ_{SR} is the micelle number concentration at the transition point.

As seen from Table 1, the effective diameter of the mixed spherical micelles, d_{EFF} , as determined by SLS, is more than 2 times larger than the hydrodynamic diameter, d_{h} , determined by DLS, which is due to the long-ranged electrostatic repulsion between the charged micelles. Note that this difference has a large impact on the effective volume fraction of the micelles in the solution, because Φ_{EFF} is proportional to $(d_{\text{EFF}})^3$. Therefore, the electrostatic repulsion between the mixed micelles significantly increases their effective volume fraction (by more than 10 times), as compared to the actual volume fraction of the micelles in the solution. As explained in refs 21–25, the effective micelle volume fraction is decisive for the magnitude of the oscillatory structure forces which stabilize foam and emulsion films from micellar solutions. Not surprisingly, we found (unpublished results) that foam films formed from mixed SDS/CAPB solutions exhibit a pronounced stratification; this would not be the case without the strong electrostatic repulsion between the micelles and the ensuing, relatively large values of d_{EFF} and Φ_{EFF} .

The effective volume fraction of the micelles at the concentration of sphere-to-rod transition, $\Phi_{\text{EFF}}(C_{\text{SR}})$, was around and below 10% for the mixed solutions with $f_{\text{CAPB}} > 0.5$; see Table 1. The driving energy for the sphere-to-rod transition in the studied systems is considered in the following section.

4. Interactions between the SDS and CAPB Molecules

The sphere-to-rod transition at $C = C_{\text{SR}}$ is driven by the difference in the interactions between the surfactant molecules and in the packing of these molecules, in the spherical and rodlike micelles. In this section, we use the light scattering data to estimate the difference between the standard chemical potentials of the surfactant molecules incorporated in spherical and rodlike micelles, $\Delta\mu_{\text{SR}}^0 \equiv \mu_{\text{R}}^0 - \mu_{\text{S}}^0$. In other words, $\Delta\mu_{\text{SR}}^0$ is the change in the average interaction energy of a surfactant molecule with its neighbors, when the molecule is transferred from a spherical into a rodlike micelle. From a thermodynamic viewpoint, $\Delta\mu_{\text{SR}}^0$ is the driving energy for the observed sphere-to-rod transition. Note that the rodlike micelles have larger aggregation numbers than the spherical ones,

(21) Kralchevsky, P. A.; Denkov, N. D. *Chem. Phys. Lett.* **1995**, *240*, 358.

(22) Nikolov, A. D.; Wasan, D. T.; Denkov, N. D.; Kralchevsky, P. A.; Ivanov, I. B. *Prog. Colloid Polym. Sci.* **1990**, *82*, 87.

(23) Wasan, D. T.; Nikolov, A. D.; Kralchevsky, P. A.; Ivanov, I. B. *Colloids Surf.* **1992**, *67*, 139.

(24) Bergeron, V.; Radke, C. J. *Langmuir* **1992**, *8*, 3020.

(25) Marinova, K. G.; Gurkov, T. D.; Dimitrova, T. D.; Alargova, R. G.; Smith, D. *Langmuir* **1998**, *14*, 2011.

Table 1. Aggregation Number; Second Virial Coefficient, A_2 ; Sphere-to-Rod Transition Concentration, C_{SR} ; Effective Micelle Volume Fraction at the Transition Concentration Calculated from Equation 7, $\Phi_{EFF}(C_{SR})$; Effective Micelle Diameter as Calculated from Equation 6, d_{EFF} ; and Hydrodynamic Diameter, d_h , as Measured by DLS, at Several Molar Fractions of CAPB in the Surfactant Mixture, f_{CAPB}

f_{CAPB}	aggregation number			virial coefficient A_2	C_{SR} , mM	$\Phi_{EFF}(C_{SR})$, %	d_{EFF} , nm	d_h , nm
	N_{SDS}	N_{CAPB}	N_S					
0 ^a	89	0	89		250	→100		4.8
0.5	58	58	116	0.002 32	35	25	13.9	4 ± 1
0.67	37	73	110	0.001 52	25	11	12.1	4.9 ± 0.5
0.75	28	86	114	0.001 29	17	6.9	11.7	5.3 ± 0.5
0.8 ^b					10			5.8 ± 1
1.0	0	84	84	0.000 56	>500		7.6	5.2 ± 0.5

^a The values for pure SDS are calculated by using literature data (refs 17, 19, and 20). ^b No SLS experiments were performed at $f_{CAPB} = 0.8$.

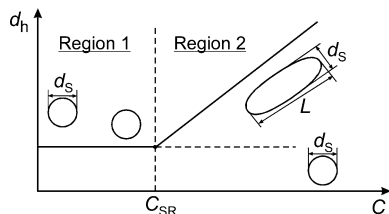


Figure 5. Schematic presentation of the surfactant aggregates in the studied solutions, according to the model used to determine the length, L , and the aggregation number, N_R , of the rodlike micelles. In the concentration range below the sphere-to-rod transition, $C < C_{SR}$, only spherical micelles with diameter d_s are present (region 1). At $C \geq C_{SR}$, spherical and rodlike micelles (possibly of different surfactant composition) are in thermodynamic equilibrium (region 2). In region 2, the diameter of the spherical micelles is assumed to be the same as in region 1 ($d_s \approx 5$ nm) and their concentration to be approximately constant and equal to C_{SR} .

which means that the sphere-to-rod transition is related to a loss of entropy (due to a decrease in the micelle number concentration) that should be compensated by a gain in the interaction energy between the molecules; hence, $\Delta\mu_{SR}^0$ should be negative.

In the region of rodlike micelles, the measured diffusion coefficient, D , is a quantity averaged over all micelles present in the solution. Furthermore, for the rodlike micelles D is averaged over their possible orientations in the solution. In the following consideration, we assume that the surfactant solution contains two types of micelles, spherical and rodlike, which are in thermodynamic equilibrium with each other, in the concentration range beyond C_{SR} (region 2 in Figure 5).²⁶ The surfactant composition of these two types of micelles is not necessarily the same; they can differ in the relative amounts of SDS and CAPB. Indeed, one can expect that the spherical micelles in region 2 can be enriched in SDS (in comparison with the surfactant composition of the entire solution), because the area per molecule in the spherical aggregates is larger; as a result, the electrostatic repulsion between the charged headgroups of SDS in spherical micelles is smaller as compared to the repulsion in rodlike micelles having the same surfactant composition. Since we have no methods to determine the exact composition of the micelles, in the subsequent considerations we use the equations for quasi-one-component surfactant aggregates. This means that the discussed chemical potentials of the surfactant molecules, incorporated in spherical or rodlike micelles, are averaged over the SDS and CAPB molecules present in the respective micelles.

(26) The coexistence of spherical and rodlike micelles was experimentally established by SANS measurements in the study by: Nakano, M.; Matsuoka, H.; Yamaoka, H.; Poppe, A.; Richter, D. *Macromolecules* **1999**, *32*, 697. The possibility for such coexistence is suggested also by the theory of surfactant self-assembly (e.g., refs 27–31 below).

The assumption that the two types of micelles (spherical and rodlike) are in equilibrium allows us to apply the thermodynamic theory of self-assembly^{17,27–30} and to estimate the difference between the standard chemical potentials of the surfactant molecules incorporated in spherical and rodlike micelles, $\Delta\mu_{SR}^0$. According to this theory, the chemical potential of the surfactant molecules incorporated in noninteracting micelles can be presented as

$$\mu_S(N_S) = \mu_S^0(N_S) + \frac{kT}{N_S} \ln(X_S/N_S) \quad (8a)$$

$$\mu_R(N_R) = \mu_R^0(N_R) + \frac{kT}{N_R} \ln(X_R/N_R) \quad (8b)$$

where $\mu_S(N_S)$ is the chemical potential of a molecule incorporated in a spherical aggregate with aggregation number N_S , and $\mu_S^0(N_S)$ is the respective standard part of the chemical potential. The quantity $X_S = C_S/(C_S + 55.5)$ is the molar fraction of surfactant incorporated in spherical aggregates, normalized by all components in the solution, including water (55.5 M is the molar concentration of water in the solutions). Respectively, X_S/N_S is the molar fraction of the spherical micelles in the solution. The subscripts S and R in eqs 8a and 8b denote quantities referring to spherical and rodlike micelles, respectively. In our consideration, we do not take explicitly into account the polydispersity of the micelles and associate N_S or N_R with the mass-averaged aggregation number of the respective types of micelles. Hence, X_S and X_R denote the total molar fraction of surfactant that is incorporated into spherical and rodlike micelles, respectively.

The assumption that the spherical and rodlike micelles are in equilibrium implies that $\mu_R = \mu_S$. From eqs 8a and 8b, one deduces the following expression for the difference between the standard chemical potentials of the surfactant molecules in spherical and rodlike micelles:

$$\Delta\mu_{RS}^0 \equiv \mu_R^0(N_R) - \mu_S^0(N_S) = kT \ln[(X_S/N_S)^{1/N_S} (N_R/X_R)^{1/N_R}] \quad (9)$$

Therefore, one could estimate $\Delta\mu_{SR}^0$ if the aggregation numbers and the concentrations of the spherical and rodlike micelles are known. Our SLS experiments showed

(27) Missel, P. J.; Mazer, N. A.; Benedek, G. B.; Young, C. Y.; Carey, M. C. *J. Phys. Chem.* **1980**, *84*, 1044. Missel, P. J.; Mazer, N. A.; Carey, M. C.; Benedek, G. B. *J. Phys. Chem.* **1989**, *93*, 8354.

(28) Israelachvili, J. N. *Intermolecular and Surface Forces*; Academic Press: New York, 1992.

(29) Alargova, R. G.; Danov, K. D.; Kralchevsky, P. A.; Broze, G.; Mehreteab, A. *Langmuir* **1998**, *14*, 4036.

(30) Alargova, R. G.; Ivanova, V. P.; Kralchevsky, P. A.; Mehreteab, A.; Broze, G. *Colloids Surf., A* **1998**, *142*, 201.

that the aggregation number of the spherical micelles in the studied mixed solutions of SDS and CAPB was virtually independent of the molar fraction of CAPB in the mixture, f_{CAPB} , when the latter was in the range between 0.5 and 0.75 ($N_{\text{S}} = 113 \pm 5$, see Table 1). For that reason, in the following estimates we assume that N_{S} is equal to 113 for all mixed solutions that were studied (the final results were not very sensitive to small changes in N_{S}). For the molar fraction of the surfactants incorporated in the spherical micelles, X_{S} , we assume that it remains approximately constant after the sphere-to-rod transition, that is, $X_{\text{S}} \approx X_{\text{SR}}$ at $X \geq X_{\text{SR}}$; here $X = C/(C + 55.5)$ is the total molar fraction of surfactant in the solution and X_{SR} is the respective fraction at the transition. Under the latter assumption, eq 9 can be transformed to read

$$\Delta\mu_{\text{RS}}^0 = kT \ln[(X_{\text{SR}}/N_{\text{S}})^{1/N_{\text{S}}}(N_{\text{R}}/(X - X_{\text{SR}}))^{1/N_{\text{R}}}] \quad (9a)$$

Therefore, one can estimate $\Delta\mu_{\text{SR}}^0$ from eq 9a if the mean aggregation number of the rodlike micelles, N_{R} , is known.

To estimate N_{R} , we approximated the shape of the rodlike micelles by an elongated ellipsoid, whose two small axes are equal to the diameter of the spherical micelles, $d_{\text{S}} \approx 5$ nm; see Figure 5. The long axis of the ellipsoid, L (the micelle length), can be estimated from the value of the mean micellar diffusion coefficient, D , which is measured by DLS. In fact, D is a mass-averaged quantity over all spherical and cylindrical micelles present in the solution. Assuming that for $C > C_{\text{SR}}$ the concentration of the spherical micelles remains equal to C_{SR} and their diameter remains equal to d_{S} , we calculated the mean diffusion coefficient of the rodlike micelles, $D_{\text{R}} = (CD - C_{\text{SR}}D_{\text{S}})/(C - C_{\text{SR}})$. From D_{R} , we calculated the length of the rodlike micelles, L , by using expressions relating the diffusion coefficient of an ellipsoid with its dimensions (see refs 18 and 29–31 for the respective theoretical expressions and procedure for analysis of DLS data for rodlike micelles). From the dimensions of the rodlike micelles, d_{S} and L , we estimated the mean volume of the micelles, $V_{\text{RM}} \approx (\pi/6)Ld_{\text{S}}^2$, and their mean aggregation number, N_{R} , at various ratios of SDS and CAPB in the mixture. In these estimates, we assumed that the molar ratio SDS/CAPB in the rodlike micelles is the same as that in the entire surfactant solution and used $V_{\text{SDS}} \approx 0.652$ nm³ and $V_{\text{CAPB}} \approx 0.881$ nm³ for the volumes of the SDS and CAPB molecules, respectively (these volumes were calculated by dividing the volume of the spherical micelle formed in the solutions of individual SDS or CAPB by the respective aggregation number, N_{S}). Finally, we estimated $\Delta\mu_{\text{SR}}^0$ for the solutions containing rodlike micelles by means of eq 9a.

Illustrative results for the increase of N_{R} with the surfactant concentration are shown in Figure 6A for two systems, $f_{\text{CAPB}} = 0.5$ ($C_{\text{SR}} \approx 35$ mM) and $f_{\text{CAPB}} = 0.8$ ($C_{\text{SR}} \approx 10$ mM). One sees that N_{R} increases linearly with C and reaches almost 10³ molecules per micelle at $(C - C_{\text{SR}}) = 50$ mM. Interestingly, we found that the results for these two systems fall very close to each other (cf. the circles and the empty squares in Figure 6A), but this could be a fortuitous coincidence, because the results for the other SDS/CAPB ratios (not shown on the figure) do not fall on the same straight line. The intercept of the linear fit, drawn through the calculated points in Figure 6A, is 104 ± 10 , which is very close to the aggregation number of the spherical micelles, as determined by SLS for concentrations $C < C_{\text{SR}}$.

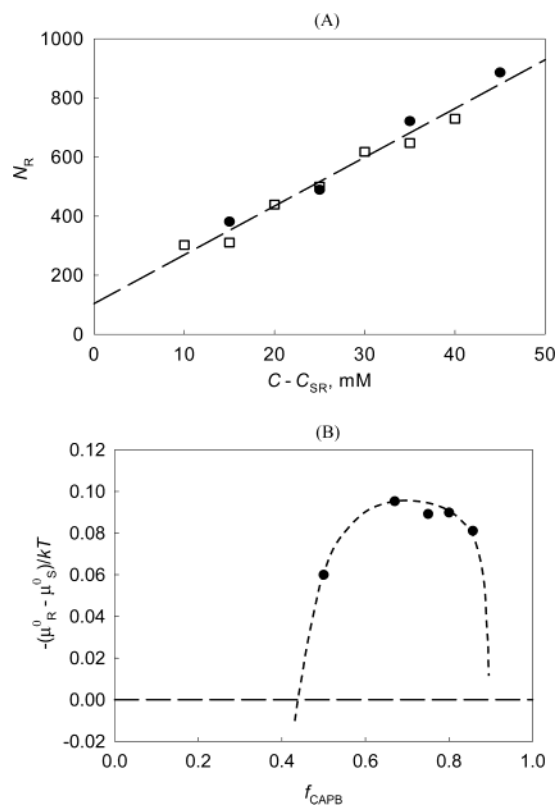


Figure 6. (A) Dependence of the aggregation number of the rodlike micelles, N_{R} , on the surfactant concentration, $(C - C_{\text{SR}})$, in mixed CAPB/SDS solutions at $f_{\text{CAPB}} = 0.5$ (circles) and 0.8 (empty squares). The straight line is a linear fit to the experimental points. (B) Difference between the standard chemical potentials of a surfactant molecule in rodlike, μ_{R}^0 , and spherical, μ_{S}^0 , micelles as a function of f_{CAPB} for $C = 40$ mM (see section 4). The dashed curve indicates the expected trend of the dependence $\Delta\mu_{\text{RS}}^0$ vs f_{CAPB} .

By using eq 9a, we estimated $\Delta\mu_{\text{SR}}^0$ to be between -0.05 and -0.1 kT per molecule for all SDS/CAPB solutions in which the sphere-to-rod transition was observed. The magnitude of $\Delta\mu_{\text{SR}}^0$ slightly increased with the raise of the total surfactant concentration, C . To make a comparison between the results for various SDS/CAPB ratios, in Figure 6B we plot the calculated value of $\Delta\mu_{\text{SR}}^0$ at a fixed total surfactant concentration, $C = 40$ mM. As seen from Figure 6B, the magnitude of $\Delta\mu_{\text{SR}}^0$ passes through a relatively flat maximum at $f_{\text{CAPB}} \approx 0.7$. To draw the dashed curve in Figure 6B, we have used the experimental fact that the sphere-to-rod transition occurs at much higher total surfactant concentration when $f_{\text{CAPB}} < 0.5$ and $f_{\text{CAPB}} > 0.85$ (that is, the dashed curve indicates the expected variation of $\Delta\mu_{\text{SR}}^0$ with f_{CAPB}).

The magnitude of $\Delta\mu_{\text{SR}}^0$ (≈ 0.1 kT) is by no means negligible, because one should multiply this value by the micelle aggregation number, N_{S} or N_{R} (which are of the order 10^2 – 10^3), to estimate the contribution of this term to the total energy of micelle formation to be 10–100 kT . Such a magnitude of $\Delta\mu_{\text{SR}}^0$ is sufficient to trigger the observed sphere-to-rod transition in the studied systems. Indeed, one can make a comparison with the “ladder model” by Missel et al.,²⁷ in which the growth of rodlike micelles in one-component surfactant solution is expressed through the equilibrium constant, K , which, in our notation, can be expressed as

$$K \equiv \exp[N_{\text{S}}\Delta\mu_{\text{RS}}^0/kT] \quad (10)$$

(31) Alargova, R.; Petkov, J.; Petsev, D.; Ivanov, I. B.; Broze, G.; Mehreteab, A. *Langmuir* **1995**, *11*, 1530.

For our systems, the exponent, $N_S \Delta \mu_{RS}^0 / kT \approx 10$, is a sufficiently large value for triggering the formation of rodlike micelles.

In the above estimates, we have neglected the interactions between the micelles in the interpretation of the data from DLS. By comparing theory and experiment, Missel et al.²⁷ have shown that these interactions become important only when

$$C/C^* \geq 0.45 \quad (11)$$

where C^* is the surfactant concentration at which the mean distance between the micelles is equal to the micelle radius of gyration, R_g . In the studied solutions, C was always below 0.1 M and the aggregation number varied between ca. 10^2 and 10^3 (largest aggregation numbers corresponding to highest concentrations). For cylindrical micelles, the radius of gyration R_g is given by the expression (e.g., ref 18)

$$R_g = (L^2/12 + d_s^2/8)^{1/2} \quad (12)$$

In our systems, $d_s \approx 5$ nm and $L \leq 50$ nm, which gives $R_g \leq 15$ nm. From the experimental data, we estimated that $C/C^* < 0.45$ in all studied micellar solutions, which allows us to neglect (as a reasonable first approximation) the interaction between the micelles in the analysis of the DLS data.

5. Conclusions

Static and dynamic light scattering experiments showed that mixed SDS/CAPB micelles undergo a sphere-to-rod transition at rather low total surfactant concentrations, ≈ 10 mM. For comparison, this transition occurs at 250 mM for pure SDS, whereas for CAPB alone, it is above 500 mM. The minimal transitional concentration was found at a molar fraction $f_{CAPB} \approx 0.8$ in the surfactant

mixture. The observed micelle transition brings about a rapid increase of the solution viscosity. From the dependence of the aggregation number on the surfactant concentration, we estimated the mean energy for transfer of a surfactant molecule from a spherical into a rodlike micelle, $\Delta \mu_{SR}^0$, to be of the order of -0.1 kT per molecule.

Parallel experiments with mixed solutions of CAPB and sodium laureth sulfate (SDP3S) showed that the sphere-to-rod transition for this mixture occurs at higher total surfactant concentrations, above 40 mM. One can explain the latter result by considering the fact that the additional ethoxy groups make the headgroup of SDP3S bulkier, as compared to SDS. As a result, the mean area per molecule in the micelles containing SDP3S is expected to be larger, which should lead to a smaller spontaneous radius of curvature of the micelles and, hence, to a less favored transition from spherical to rodlike micelles.

The data for the aggregation number and the second osmotic virial coefficient of the spherical micelles, measured by SLS, were used to calculate the effective micelle diameter, which includes a contribution from the long-range electrostatic repulsion between the micelles. This effective diameter was found to be about 2 times larger than the hydrodynamic one. The respective large effective volume fraction of the micelles promotes pronounced colloidal structural forces, created by the repelling micelles, in foam and emulsion films formed from mixed SDS/CAPB solutions (unpublished results).

Acknowledgment. This study was supported by the Unilever Research Center, Edgewater, NJ. Some of the calculations were performed and several of the figures were prepared by Dr. S. Tcholakova (University of Sofia); her help is gratefully acknowledged.

LA035717P